REPORT DOCUMENTATION PAGE

Form Approved OMB NO. 0704-0188

1. REPORT DATE (DD-MM-YYYY)	2. REPORT TYPE	3. DATES COVERED (From - To)
09-11-2014	Final Report	10-Aug-2010 - 9-Aug-2013

4. TITLE AND SUBTITLE
Final Report: Magneto-electric Coupling in Domain Engineered Multiferroic Thin Film Heterostructures

5a. CONTRACT NUMBER
W911NF-10-1-0362

5b. GRANT NUMBER

5c. PROGRAM ELEMENT NUMBER
611102

6. AUTHORS
Chang-Beom Eom

5d. PROJECT NUMBER

5e. TASK NUMBER

5f. WORK UNIT NUMBER

7. PERFORMING ORGANIZATION NAMES AND ADDRESSES
University of Wisconsin - Madison
Suite 6401
21 N Park St
Madison, WI 53715 -1218

8. PERFORMING ORGANIZATION REPORT NUMBER

9. SPONSORING/MONITORING AGENCY NAME(S) AND ADDRESS (ES)
U.S. Army Research Office
P.O. Box 12211
Research Triangle Park, NC 27709-2211

10. SPONSOR/MONITOR'S ACRONYM(S)
ARO

11. SPONSOR/MONITOR'S REPORT NUMBER(S)
56987-MS.26

12. DISTRIBUTION AVAILIBILITY STATEMENT
Approved for Public Release; Distribution Unlimited

13. SUPPLEMENTARY NOTES
The views, opinions and/or findings contained in this report are those of the author(s) and should not contrued as an official Department of the Army position, policy or decision, unless so designated by other documentation.

14. ABSTRACT
Epitaxial BiFeO3 (BFO) thin films have potential for designing novel magneto-electric devices if their unrivaled room-temperature multiferroic properties can be exploited in exchange-coupling. Until now, the fundamental problem in implementing these devices is that exchange interactions between BFO and a ferromagnetic overlayer have been observed only in the presence of domain walls that are also responsible for high leakage currents during electrical poling of the BFO. We have new evidence that the existence of an intrinsic exchange interaction between BFO and a cobalt overlayer that is not mediated by domain walls, and that provides an alternative solution the

15. SUBJECT TERMS
Magnetoelectric Coupling, Multiferroic, Thin Films

16. SECURITY CLASSIFICATION OF:			17. LIMITATION OF ABSTRACT	15. NUMBER OF PAGES	19a. NAME OF RESPONSIBLE PERSON
a. REPORT	b. ABSTRACT	c. THIS PAGE			Chang-Beom Eom
UU	UU	UU	UU		19b. TELEPHONE NUMBER 608-263-6305

Report Title

Final Report: Magneto-electric Coupling in Domain Engineered Multiferroic Thin Film Heterostructures

ABSTRACT

Epitaxial BiFeO3 (BFO) thin films have potential for designing novel magneto-electric devices if their unrivaled room-temperature multiferroic properties can be exploited in exchange-coupling. Until now, the fundamental problem in implementing these devices is that exchange interactions between BFO and a ferromagnetic overlayer have been observed only in the presence of domain walls that are also responsible for high leakage currents during electrical poling of the BFO. We have new evidence that the existence of an intrinsic exchange interaction between BFO and a cobalt overlayer that is not mediated by domain walls, and that provides an alternative solution the implementation of these devices. The intrinsic exchange coupling relies on the use of monodomain BFO films, and has shown the capability to rotate the magnetization of a cobalt overlayer by switching the electrical polarization of BFO.

Enter List of papers submitted or published that acknowledge ARO support from the start of the project to the date of this printing. List the papers, including journal references, in the following categories:

(a) Papers published in peer-reviewed journals (N/A for none)

Received		Paper
09/08/2011	2.00	Christopher T. Nelson, Benjamin Winchester, Yi Zhang, Sung-Joo Kim, Alexander Melville, Carolina Adamo, Chad M. Folkman, Seung-Hyub Baek, Chang-Beom Eom, Darrell G. Schlom, Long-Qing Chen, Xiaoqing Pan. Spontaneous Vortex Nanodomain Arrays at Ferroelectric Heterointerfaces, Nano Letters, (02 2011): 0. doi: 10.1021/nl1041808
09/08/2011	7.00	J. W. Park, S. H. Baek, P. Wu, B. Winchester, C. T. Nelson, X. Q. Pan, L. Q. Chen, T. Tybell, C. B. Eom. Origin of suppressed polarization in BiFeO[sub 3] films, Applied Physics Letters, (11 2010): 0. doi: 10.1063/1.3506902
09/08/2011	6.00	J. F. Ihlefeld, C. M. Folkman, S. H. Baek, G. L. Brennecka, M. C. George, J. F. Carroll, C. B. Eom. Effect of domain structure on dielectric nonlinearity in epitaxial BiFeO[sub 3] films, Applied Physics Letters, (12 2010): 0. doi: 10.1063/1.3533017
09/08/2011	5.00	T. H. Kim, S. H. Baek, S. Y. Jang, S. M. Yang, S. H. Chang, T. K. Song, J.-G. Yoon, C. B. Eom, J.-S. Chung, T. W. Noh. Step bunching-induced vertical lattice mismatch and crystallographic tilt in vicinal BiFeO[sub 3](001) films, Applied Physics Letters, (01 2011): 0. doi: 10.1063/1.3535981
09/08/2011	4.00	Seung-Hyub Baek, Chad M. Folkman, Jae-Wan Park, Sanghan Lee, Chung-Wung Bark, Thomas Tybell, Chang-Beom Eom. The Nature of Polarization Fatigue in BiFeO3, Advanced Materials, (04 2011): 0. doi: 10.1002/adma.201003612
09/08/2011	1.00	Ji Young Jo, Pice Chen, Rebecca J. Sichel, Seung-Hyub Baek, Ryan T. Smith, Nina Balke, Sergei V. Kalinin, Martin V. Holt, Jo?rg Maser, Kenneth Evans-Lutterodt, Chang-Beom Eom, Paul G. Evans. Structural Consequences of Ferroelectric Nanolithography, Nano Letters, (08 2011): 0. doi: 10.1021/nl2009873
09/08/2011	3.00	T. H. Kim, S. H. Baek, S. M. Yang, Y. S. Kim, B. C. Jeon, D. Lee, J.-S. Chung, C. B. Eom, J.-G. Yoon, T. W. Noh. Polarity-dependent kinetics of ferroelectric switching in epitaxial BiFeO3(111) capacitors, Applied Physics Letters, (07 2011): 0. doi: 10.1063/1.3609235
11/08/2014	8.00	Kara J. Manke, A. A. Maznev, Christoph Klieber , Keith A. Nelson, Seung Hyub Baek, Chang-Beom Eom. Coherent Brillouin spectroscopy in a strongly scattering liquid by picosecond ultrasonics, Optics Letters, (08 2011): 2925. doi:
11/08/2014	18.00	J. D. Burton, H. Lu, T. A. George, Y. Wang, I. Ketsman, C.-W. Bark, S. Ryu, D. J. Kim, J. Wang, C. Binek, P. A. Dowben, A. Sokolov, C.-B. Eom, E. Y. Tsymbal, A. Gruverman. Electric modulation of magnetization at the BaTiO3/La0.67Sr0.33MnO3 interfaces , Appl. Phys. Lett., (06 2012): 232904. doi:
11/08/2014	17.00	X.Q. Pan, Y.M. Liu, J.Y. Li, C.B. Eom, E. Wang, P. Gao, C.T. Nelson, J.R. Jokisaari, Y. Zhang, S.H. Baek, C.W. Bark. Direct Observations of Retention Failure in Ferroelectric Memories , Advanced Materials, (02 2012): 1106. doi:
11/08/2014	16.00	Pice Chen, Rebecca J. Sichel, Ji Young Jo, Ryan T. Smith, Chang-Beom Eom, Osami Sakata, Eric M. Dufresne, Paul G. Evans. Nonlinearity in the high-electric-field piezoelectricity of epitaxial BiFeO3 on SrTiO3 , Appl. Phys. Lett., (02 2012): 62906. doi:

11/08/2014 15.00 D. Lee, S.M. Yang, T.H. Kim, B.C. Jeon, Y.S. Kim, J.G. Yoon, H.N. Lee, S.H. Baek, C.B. Eom, T.W. Noh. Multilevel Data Storage Memory Using Deterministic Polarization Control ,
Advanced Materials, (01 2012): 402. doi:

11/08/2014 14.00 S.O. Hruszkewycz, C.M. Folkman, M.J. Highland, M.V. Holt, S.H. Baek, S.K. Streiffer, P. Baldo, C.B. Eom, P.H. Fuoss. X-ray nanodiffraction of tilted domains in a poled epitaxial BiFeO3 thin film ,
Appl. Phys. Lett., (12 2012): 232903. doi:

11/08/2014 13.00 P. Gao, C.T. Nelson, J.R. Jokisaari, S.H. Baek, C.W. Bark, Y. Zhang, E.G. Wang, D.G. Schlom, C.B. Eom, X.Q. Pan. Revealing the role of defects in ferroelectric switching with atomic resolution,
Nature Communications, (12 2012): 591. doi:

11/08/2014 12.00 P. Gao, J. R. Jokisaari, C. Heikes, C. Adamo, A. Melville, S.H. Baek, C.T. Nelson, C.M. Folkman, B. Winchester, Y. Gu, Y. Liu, K. Zhang, E. Wang, J. Li, L.Q. Chen, C. B, Eom, D. G. Schlom, Xiaoqing Pan. Domain Dynamics during Ferroelectric Switching,
Science, (11 2011): 968. doi:

11/08/2014 11.00 Chad M. Folkman, Seung-Hyub Baek, Chang-Beom Eom. Twin wall distortions through structural investigation of epitaxial BiFeO3 thin films ,
J. Mat. Res, 26, 2844 (2011), (11 2011): 2844. doi:

11/08/2014 10.00 S. H. Baek, T. H. Kim,, J.-G. Yoon, C. M. Folkman, C. B. Eom, T. W. Noh, D. Lee. Polarity control of carrier at ferroelectric/metal interfaces for electrically switchable diode and photovoltaic effects,
Physical Review B, (09 2011): 125305. doi:

11/08/2014 9.00 Paul G. Evans, Ji Young Jo, Pice Chen, Rebecca J. Sichel, Seung-Hyub Baek , Ryan T. Smith, Nina Balke, Sergei V. Kalinin, Martin V. Holt, Jörg Maser? , Kenneth Evans-Lutterodt , Chang-Beom Eom. Structural consequences of ferroelectric nanolithography,
Nano Letters, (07 2011): 3080. doi:

11/09/2014 25.00 D. W. Jeong, Hong Chul Choi, Choong H. Kim, Seo Hyoung Chang, C. H. Sohn, H. J. Park, T. D. Kang, Deok-Yong Cho, S. H. Baek, C. B. Eom, J. H. Shim, J. Yu, K. W. Kim, S. J. Moon, T. W. Noh. Temperature Evolution of Itinerant Ferromagnetism in SrRuO_{3} Probed by Optical Spectroscopy,
Physical Review Letters, (06 2013): 0. doi: 10.1103/PhysRevLett.110.247202

11/09/2014 19.00 C. B. Eom, S. H. Baek. Reliable polarization switching of BiFeO3,
Philosophical Transactions of the Royal Society A: Mathematical, Physical and Engineering Sciences, (09 2012): 0. doi: 10.1098/rsta.2012.0197

11/09/2014 20.00 A. Gruverman, D. J. Kim, H. Lu, S. Ryu, C.-W. Bark, C.-B. Eom, E. Y. Tsymbal. Ferroelectric Tunnel Memristor,
Nano Letters, (11 2012): 0. doi: 10.1021/nl302912t

11/09/2014 21.00 Tae Won Noh, Taeyoon Min, Sang Mo Yang, Daesu Lee, Yong Su Kim, Seung-Hyub Baek, Wittawat Saenrang, Chang-Beom Eom, Tae Kwon Song, Jong-Gul Yoon, Byung Chul Jeon, Tae Heon Kim. Continuous Control of Charge Transport in Bi-Deficient BiFeO Films Through Local Ferroelectric Switching,
Advanced Functional Materials, (12 2012): 0. doi: 10.1002/adfm.201201490

11/09/2014 22.00 Seung Hyub Baek, Sang Mo Yang, Yeong Jae Shin, Tae Heon Kim, Yong Su Kim, Jong-Gul Yoon, Tae Won Noh, Chang Beom Eom, Daesu Lee, Byung Chul Jeon. Active Control of Ferroelectric Switching Using Defect-Dipole Engineering,
Advanced Materials, (12 2012): 0. doi: 10.1002/adma.201203101

11/09/2014 23.00 S. Cao, P. Liu, J. Tang, H. Lu, C.-W. Bark, S. Ryu, C. B. Eom, A. Gruverman, P. A. Dowben. Magnetoelectric coupling at the EuO/BaTiO3 interface,
Applied Physics Letters, (2013): 0. doi: 10.1063/1.4803492

11/09/2014 24.00 Seung-Hyub Baek, Chang-Beom Eom. Epitaxial integration of perovskite-based multifunctional oxides on silicon,
Acta Materialia, (05 2013): 0. doi: 10.1016/j.actamat.2012.09.073

TOTAL: 25

Number of Papers published in peer-reviewed journals:

(b) Papers published in non-peer-reviewed journals (N/A for none)

Received Paper

TOTAL:

Number of Papers published in non peer-reviewed journals:

(c) Presentations

Number of Presentations: 0.00

Non Peer-Reviewed Conference Proceeding publications (other than abstracts):

Received Paper

TOTAL:

Number of Non Peer-Reviewed Conference Proceeding publications (other than abstracts):

Peer-Reviewed Conference Proceeding publications (other than abstracts):

Received Paper

TOTAL:

Number of Peer-Reviewed Conference Proceeding publications (other than abstracts):

(d) Manuscripts

Received Paper

TOTAL:

Number of Manuscripts:

Books

Received Book

TOTAL:

Received Book Chapter

TOTAL:

Patents Submitted

Patents Awarded

Awards

1. The PI, Chang-Beom Eom has been appointed to Wisconsin Alumni Research Foundation Named Professorship in 2013.

2. The PI, Chang-Beom Eom has been appointed to Harvey D. Spangler Distinguished Professorships in 2013.

3. Chang-Beom Eom as been severed as an Associate Editor of APL Materials

4. The PI, Chang-Beom Eom, was elected as the Board of Directors of Materials Research Society (2012)

5. The PI, Chang-Beom Eom, was selected as a fellow of the Materials Research Society (2011.

6. The PI, Chang-Beom Eom, was a meeting chair of the 2011 Spring MRS meeting.

7. Seung-Hyub Baek, Graduate Student Award, received a Silver Medal, at the 2010 Materials Research Society Fall Meeting in Boston.

Graduate Students

NAME	PERCENT_SUPPORTED	Discipline
Alyssa Frey	0.50	
Wittawat Saenrang	1.00	
Morgan Baima	0.50	
FTE Equivalent:	**2.00**	
Total Number:	**3**	

Names of Post Doctorates

NAME	PERCENT_SUPPORTED
Seung-Hyub Baek	1.00
Wan-Joo Maeing	0.30
Kyouhyun Kim	0.20
FTE Equivalent:	**1.50**
Total Number:	**3**

Names of Faculty Supported

NAME	PERCENT_SUPPORTED	National Academy Member
Chang-Beom Eom	0.05	
Mark Rzchowski	0.00	
FTE Equivalent:	**0.05**	
Total Number:	**2**	

Names of Under Graduate students supported

NAME	PERCENT_SUPPORTED
FTE Equivalent:	
Total Number:	

Student Metrics

This section only applies to graduating undergraduates supported by this agreement in this reporting period

The number of undergraduates funded by this agreement who graduated during this period: 0.00

The number of undergraduates funded by this agreement who graduated during this period with a degree in science, mathematics, engineering, or technology fields:..... 0.00

The number of undergraduates funded by your agreement who graduated during this period and will continue to pursue a graduate or Ph.D. degree in science, mathematics, engineering, or technology fields:..... 0.00

Number of graduating undergraduates who achieved a 3.5 GPA to 4.0 (4.0 max scale):..... 0.00

Number of graduating undergraduates funded by a DoD funded Center of Excellence grant for Education, Research and Engineering:..... 0.00

The number of undergraduates funded by your agreement who graduated during this period and intend to work for the Department of Defense 0.00

The number of undergraduates funded by your agreement who graduated during this period and will receive scholarships or fellowships for further studies in science, mathematics, engineering or technology fields: 0.00

Names of Personnel receiving masters degrees

NAME
Morgan Baima
Total Number: 1

Names of personnel receiving PHDs

NAME
Total Number:

Names of other research staff

NAME	PERCENT_SUPPORTED
FTE Equivalent:	
Total Number:	

Sub Contractors (DD882)

Inventions (DD882)

Scientific Progress

Nature of polarization fatigue in BiFeO3

We have studied intrinsic polarization fatigue depending on the switching path using monodomain epitaxial BiFeO3 thin films. We controlled each switching path selectively by using different orientations of BiFeO3 films. The 180° switching path in (111)pc films turned out to be vulnerable to fatigue while 71° switching in (001)pc and 109° switching in (110)pc were fatigue-resistant. Our microscopic analysis with PFM showed direct evidence of the pinned domain walls with non-neutral configuration of polarization, which is consistent with macroscopic analysis of polarization fatigue using XRD and electrical measurements. We proposed a model that the complex multi-step switching process of 180° polarization reversal results in domain wall pinning by incorporation of mobile charge carriers into non-neutral domain walls. This work provides a framework for understanding electric fatigue in BiFeO3, and other low symmetric materials with complex switching routes. In addition, this work provides design rules for the reliable performance of multifunctional devices controlled by polarization switching.

Spontaneous Vortex Nanodomain Arrays at Ferroelectric Heterointerfaces

The polarization of the ferroelectric BiFeO3 subjected to different electrical boundary conditions by heterointerfaces is imaged with atomic resolution using a spherical aberration-corrected transmission electron microscope. We have found a self-assembled array of ferro-electric vortex domains near the interface between a BiFeO3 thin film and an insulating TbScO3 substrate. The driving force for their formation is localized electrostatic energies where 109o domain walls terminate at the interface. The polarization closure is observed by mapping the electric polarization with atomic resolution via HRTEM images and exhibits non-bulk characteristics such as mixed Ising-N'eel type domain walls and in-plane polarization up to twice that of the bulk film. Through comparison with phase-field simulations, we infer the presence and absence of free charge carriers at the film/air interface and the film/substrate interface, respectively. Using such an approach, atomic-scale polarization imaging can be applied to study the influence of other defects and interfaces on the properties of ferroelectric materials.

Origin of suppressed polarization in BiFeO3 films

We have studied the origin of suppressed remanent polarization in 4-variant BiFeO3 by correlating microscopic observations of ferroelectric/ferroelastic domain structures and ferroelectric measurements of (001) epitaxial BiFeO3 thin films with 2- and 4-ferroelastic domain variants. Piezoelectric force microscopy revealed that domain wall pinning was the cause of the reduced polarization observed in 4-variant BiFeO3. Using repetitive switching, the unswitched domains were completely switched and the remanent polarization reached a value comparable to 2-variant BiFeO3. These results demonstrate that control of ferroelastic domains in rhombohedral systems is necessary in order to obtain high performance and reliable ferroelectric and magnetoelectric devices.

Technology Transfer

1. Nature of Polarization Fatigue in $BiFeO_3$

As a room-temperature multiferroic, $BiFeO_3$ has been intensively investigated for non-volatile ferroelectric device applications. $BiFeO_3$, having a rhombohedral unit cell, and has the largest remanent polarization (P_r ~100 μC/cm^2) along the [111] polar direction among all known ferroelectrics, which is a promising feature as a lead-free material for ferroelectric and piezoelectric devices. Utilizing the large remanent polarization of $BiFeO_3$ would enable further reduction of the cell size limited by conventional piezoelectric and ferroelectrics such as $BaTiO_3$ and $Pb(Zr,Ti)O_3$.

Ferroelectric devices are controlled by polarization switching by an applied electric field. Due to the rhombohedral symmetry of $BiFeO_3$, there are four ferroelastic variances and three different polarization switching events: (1) 71° switching from $r1^-$ to $r3^+$, (2) 109° switching from $r1^-$ to $r2^+$ (or $r4^+$), and (3) 180° switching from $r1^-$ to $r1^+$ (the superscript + and - stand for up and down polarization, respectively). A degradation of the ferroelectric properties of $BiFeO_3$ will result in losing information storage in ferroelectric and piezoelectric devices. Especially, polarization fatigue will directly restrict the reliability of the actual devices. Hence it is important to understand the intrinsic fatigue behavior of each polarization switching path in $BiFeO_3$ thin films. We first reported that polarization fatigue in $BiFeO_3$ depends on switching path, and proposed a fatigue model which will broaden our understanding of the fatigue phenomenon in low-symmetry materials.

In order to study the intrinsic behavior of switching-path dependent fatigue, it is crucial (1) to control a single polarization switching path among the three possible ones (71°, 109° and 180°) during switching cycles and (2) to remove the extrinsic effects of the pre-existing domain or grain boundaries affecting polarization switching. To solve the latter issue, we used *monodomain* epitaxial $BiFeO_3$ thin films as a model system, without the extrinsic effects of pre-existing domain walls. In order to achieve the former requirement, we used *three different crystallographic orientations*, $(001)_{pc}$, $(110)_{pc}$ and $(111)_{pc}$, of epitaxial monodomain $BiFeO_3$ films in the vertical capacitor structure of Pt top and $SrRuO_3$ bottom electrodes (the subscript "pc" stands for pseudocubic).

Figure 2a-c show *P-E* measurements before and after the fatigue cycling of the $(001)_{pc}$, $(110)_{pc}$ and $(111)_{pc}$ $BiFeO_3$ films, respectively. Figure 2d depicts the switched polarization versus the number of switching cycles. Initial ~115 μC/cm^2 of P_r in mono-domain $(111)_{pc}$ $BiFeO_3$ film starts to degrade at ~10^4 cycles, and reduces to ~57 μC/cm^2 at 10^6 cycles. On the contrary, P_r of mono-domain $(001)_{pc}$ and $(110)_{pc}$ $BiFeO_3$ films continues unabated even up to 10^6 cycles, the maximum number of cycles in this study. This result suggests that 180° switching in $(111)_{pc}$ $BiFeO_3$ films is not favorable for a real device in terms of the reliability issue even though this has the largest remanent polarization.

We performed macroscopic analysis on $(111)_{pc}$ $BiFeO_3$ films. Figure 3a and 3b show the RSM around the 113 $SrTiO_3$ peak before and after fatigue cycles were applied to a $(111)_{pc}$ monodomain $BiFeO_3$ film, respectively. The additional peaks for $BiFeO_3$ indicate that new ferroelastic domains formed during fatigue cycles and that fatigued $(111)_{pc}$ $BiFeO_3$ films have four ferroelastic variances. It should be noted that these new ferroelastic domains are *nucleated from the initial monodomain state* with fatigue. We also investigated the microscopic domain structure using PFM to understand the configuration of new ferroelastic domains as well as to obtain local information related to electrical data of $(111)_{pc}$ $BiFeO_3$ films. We applied 10^5 switching cycles on $(111)_{pc}$ $BiFeO_3$ film with the final polarity pointing upward. The Pt top electrode was subsequently removed by ultrasonification, and the domain structure analyzed with PFM. The as-grown $(111)_{pc}$ monodomain $BiFeO_3$ film does not show any contrasts in out-of-plane (OP) and in-plane (IP) PFM images (figure 3c, d). However, PFM images of fatigued $(111)_{pc}$ $BiFeO_3$ film show contrasts coming from new domains in figure 3e (OP) and 2f (IP). The

OP image has three different contrasts: dark, grey and bright. On the other hand, the $(001)_{pc}$ and $(110)_{pc}$ monodomain $BiFeO_3$ films do not show any PFM contrasts from new domains. within ±10% error as measured by PFM on five different areas of 5 μm × 5 μm within a fatigued capacitor. Hence, it is concluded that polarization fatigue of $(111)_{pc}$ $BiFeO_3$ is directly related to the formation of new domains.

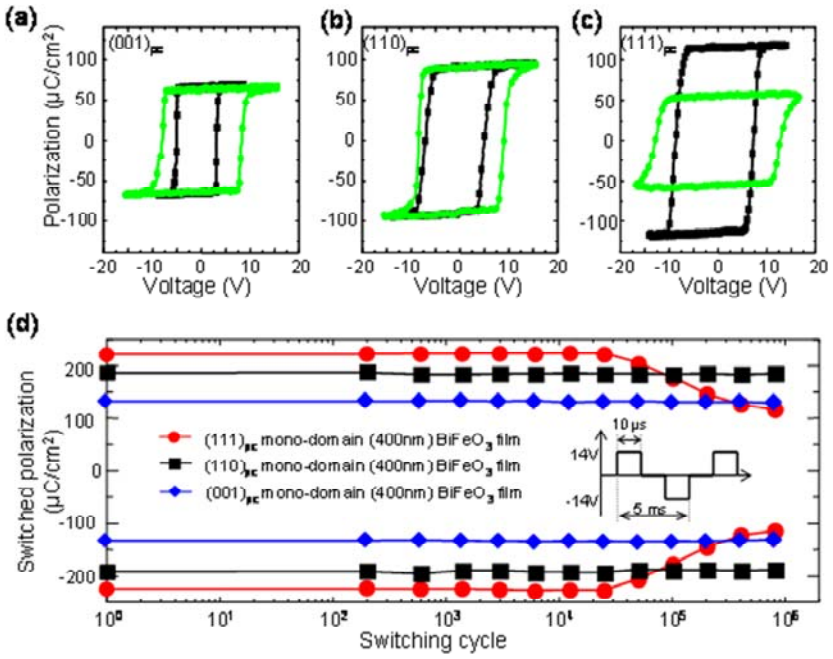

Figure 2 *P-E* hysteresis loop measurement of initial (black square) and after fatigue cycles (green circle) of a) $(001)_{pc}$, b) $(110)_{pc}$ and c) $(111)_{pc}$ 400-nm-thick monodomain $BiFeO_3$ films with Pt top and $SrRuO_3$ bottom electrodes. d) Fatigue behavior of monodomain $BiFeO_3$ films with the three different orientations. The inset shows the electrical fatigue stress profile.

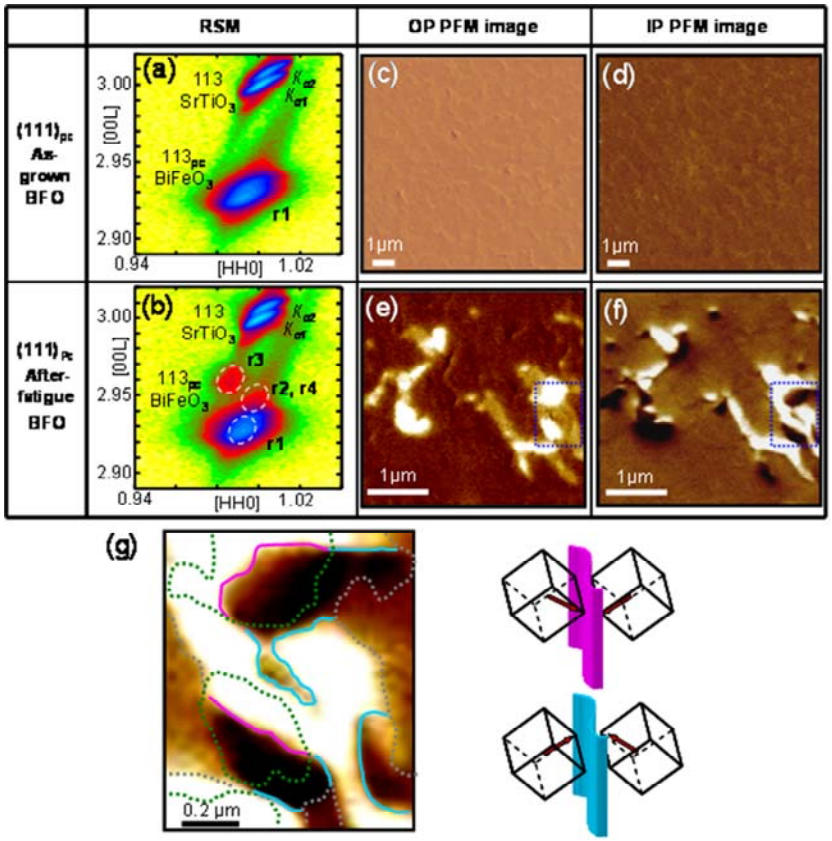

Figure 3. RSM data around the 113 $SrTiO_3$ peak of a) as-grown and b) fatigued $(111)_{pc}$ $BiFeO_3$ film. c) Out-of-plane and d) in-plane PFM image of the as-grown $(111)_{pc}$ $BiFeO_3$ film. e) Out-of-plane and f) in-plane PFM image of the $(111)_{pc}$ $BiFeO_3$ capacitor after 10^5 cycles. g) Zoomed-in IP PFM image of the blue dotted square in e) and f). Green and grey dotted lines correspond to bright and grey contrasts in the OP image, respectively. Sky-blue and pink solid lines are non-neutral domain walls, the structures of which are also illustrated on the left, respectively.

2. Exchange bilayer device geometry incorporating monodomain BFO film

We have studied the exchange coupling between the multiferroic BFO thin film and a ferromagnetic (F) overlayer such as cobalt (Co) by synchrotron techniques as shown in Fig. 4. Epitaxial monodomain BFO is grown on a miscut STO (001) substrate, resulting in a poled-down configuration. Following this, a thin layer of Co (~5 nm) is deposited on the BFO by room-temperature sputtering in 200 Oe magnetic field, followed by a passivating layer of Au (~5 nm). The structure is subsequently patterned by photolithography and ion milling to define a mesa with dimensions 200x700 μm^2; these dimensions are sufficiently large to permit focusing of the synchrotron beam (100x100 μm^2) onto the mesa at grazing incidence. Additional metallization is performed by depositing a 200x200 μm^2 layer of Pt on one corner of the mesa. The patterned wafer is mounted on a chip carrier, and the top and bottom electrodes (Pt/Au/Co and SRO, respectively) are wire-bonded to chip carrier pads to allow for *in situ* poling during the synchrotron measurements.

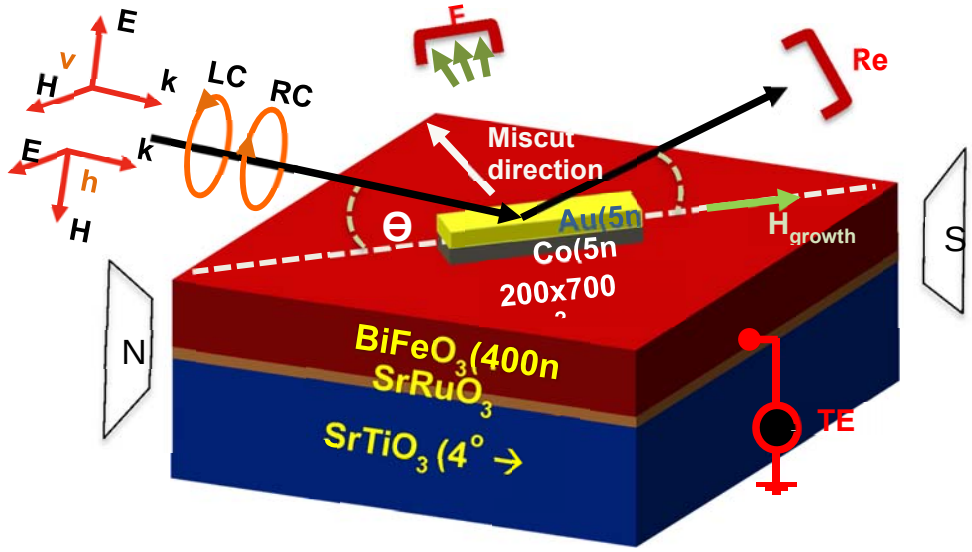

Fig. 4. Bilayer geometry for synchtrotron measurements. The long axis of the mesa is aligned with the incident photon beam (black arrows) during measurements, and the magnetic field is applied along this axis. The photon beam is incident on the sample at an angle θ, and can be polarized either circularly (left-hand circular (lcp) or right-hand circular (rcp)) or linearly (horizontal (hp) or vertical (vp)). The photon energy can be tuned in the soft X-ray range corresponding to the $L_{2,3}$ absorption resonances of Fe (~710 eV) or Co (770 eV). The absorption signal can be measured simultaneously in total electron yield (TEY), fluorescence yield (FY) and reflectivity modes. The probing depth in TEY mode is ~3-4nm, and the attenuation length at the Fe resonance is ~100 nm. This makes the TEY signal sensitive to the Co/BFO interfacial region while the fluorescence and reflectivity signals are sensitive to the bulk of the BFO film when measuring at the Fe $L_{2,3}$ absorption resonance. The synchrotron measurements were performed at the Advanced Photon Source in Argonne National Laboratory (IL) at beamline 4-ID-C in collaboration with J. W. Freeland.

The scope of the synchrotron measurements is to measure the changes of 1) the Co magnetization and 2) the AF axis orientation in the BFO film, before and after poling. This is

indicated schematically in Fig. 5. The Co magnetization (amplitude and orientation) is characterized by XMCD measurements at the Co $L_{2,3}$ edge, and the AF axis orientation of the BFO is characterized by XMLD measurements at the Fe $L_{2,3}$ edge. Both XMCD and XMLD techniques rely on on X-ray absorption spectroscopy (XAS), in which photons are absorbed through ejection of core electrons in chosen atoms (Co or Fe 2p electrons, in this case) into unoccupied states in the conduction band of the solid (3d bands above the Fermi level, in this case). The number of photons absorbed will depend on the density of available final states that is described by the dipole selection rules for the specific transition. Since the dipole selection rules are dependent on the electron spin of the initial and final states, that in turn depend on the magnetic state of the solid, XMCD can detect if the global magnetization of a ferromagnetic (F) layer (here Co) has changed its amplitude or orientation with respect to the incident photon wavevector. Since XMCD is a first-order process, the XMCD signal will be proportional to the (vector) magnetization, that is, its amplitude and direction; if the magnetization rotates during BFO poling, this will appear as a reduction of the XMCD signal by $\cos\theta$, where θ is the angle of rotation. In contrast, XMLD is well-suited to monitor the orientation of the AF axis in an AF material (which has no net magnetization averaged over many cells of the material), since it is a second-order process in which the XMLD signal is proportional to the modulus of the magnetization (or $|M^2|$). In particular, the intensity of the XMLD signal will be a maximum when the electric field vector of the photon is aligned parallel to the AF axis in one of the two linear polarization states. Hence, any change of the AF axis orientation upon poling will change the incidence geometry in which the maximum XMLD is observed.

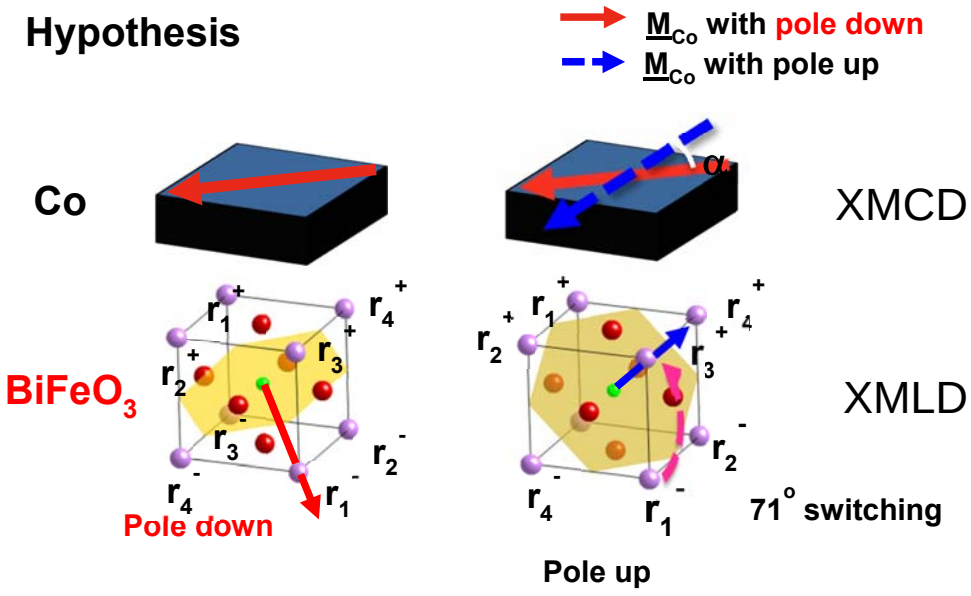

Fig. 5. XMCD and XMLD measurements to characterize the magnetic states of the bilayer: XMCD to monitor the F layer (Co), XMLD to monitor the AF layer (monodomain BFO). It has already been established in BFO single crystals that within a single ferroelastic domain the AF axis lies within an easy plane (shaded yellow) that is orthogonal to the direction of the electric polarization *P* (red or blue arrows) that is along the body diagonal of the pseudocubic unit cell. Upon poling, P will change direction (indicated above by a 71° switching event) and the AF easy plane will adjust accordingly. If the magnetization *M* of the Co layer is exchange-coupled to the AF ordering in the BFO layer, then movement of the AF plane should result in movement of *M* in the Co layer. Changes of the Co magnetization will be tracked by XMCD measurements, while changes in the orientation of the AF axis in the BFO will be tracked by XMLD measurements.

The key to this experiment, and to any potential real device, is the use of monodomain BFO films, in which there is only one ferroelastic domain (instead of 4 as shown by a 4-domain BFO film). This property of monodomain BFO ensures a 1-to-1 correspondence between the polarization direction *P* and the AF axis, and hence permits a 1-to-1 correspondence between the AF axis direction and the magnetization *M* of the ferromagnetic layer. The definite correlation between P and M is essential for any practical device. In addition, the vertical structure of the bilayer geometry ensures a low switching field, also essential for a working device.

3. Exchange coupling between monodomain BFO and Co overlayer by X-ray magnetic circular dichroism (XMCD) between 30-300 K

Exchange coupling between a monodomain BFO film and a Co overlayer was explored more carefully by XMCD at temperatures of 30 K, 150 K and 300 K. The two principle advantages of XMCD over MOKE are 1) the elemental specificity of XMCD that allows, for example, to distinguish between a net magnetization in either Co or Fe in the BFO; and 2) the quantitative nature of the XMCD signal that permits. The sample insert at beamline 4-ID-C permits *in situ* poling of the BFO (with up to 4 independent electrical contacts for 4 separate samples), so that XMCD and XMLD measurements can be performed without bringing the sample out of vacuum in order to pole the BFO. In addition, the insert can be cooled with liquid helium, allowing the sample to reach a minimum temperature near 30 K.

Room temperature measurements of XMCD and hysteresis in the monodomain Co/BFO bilayer. As shown in Fig. 6, at 300 K a large XMCD signal in the Co overlayer of ~35% was seen, along with a sharp hysteresis loop with an H_{Coerc}~ Oe. Furthermore, no change in the hysteresis loops or magnitude of the XMCD signal were visible upon switching the BFO poling from down to up. This result implies the absence of exchange coupling between the AF interfacial spin moments in the BFO and the Co magnetization.

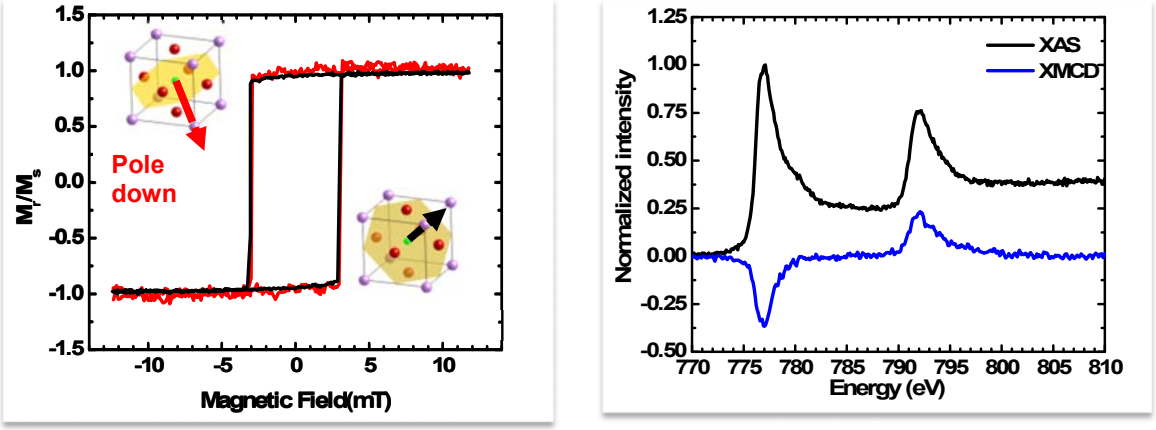

Fig. 6. XMCD and magnetic hysteresis of Co layer at room temperature.

30 K measurements of XMCD and hysteresis in the monodomain Co/BFO bilayer.

At 30 K, the evidence of exchange coupling between the BFO and Co is clear, and reveal a ~20° rotation of the Co magnetization upon switching of the BFO poling state that is robust and

repeatable. From the hysteresis loops shown in Fig. 7, a sharp hysteresis loop in the poled-down state changes to a "flattened" loop in the poled-up state. This is evidence that the magnetic easy axis in the Co layer changes upon poling, i.e., in the poled-down state the magnetic easy axis of Co is aligned with the long axis of the 200x700 μm^2 mesa, while in the poled-up state the magnetization easy direction is pulled away from its previous orientation and is pinned by the exchange coupling. This interpretation of the hysteresis loop data is confirmed by the reduction of ~8% in the XMCD amplitude, a value that corresponds to a rotation of the Co magnetization of ~20° with respect to its previous poled-down orientation (since the photon incidence angle is fixed).

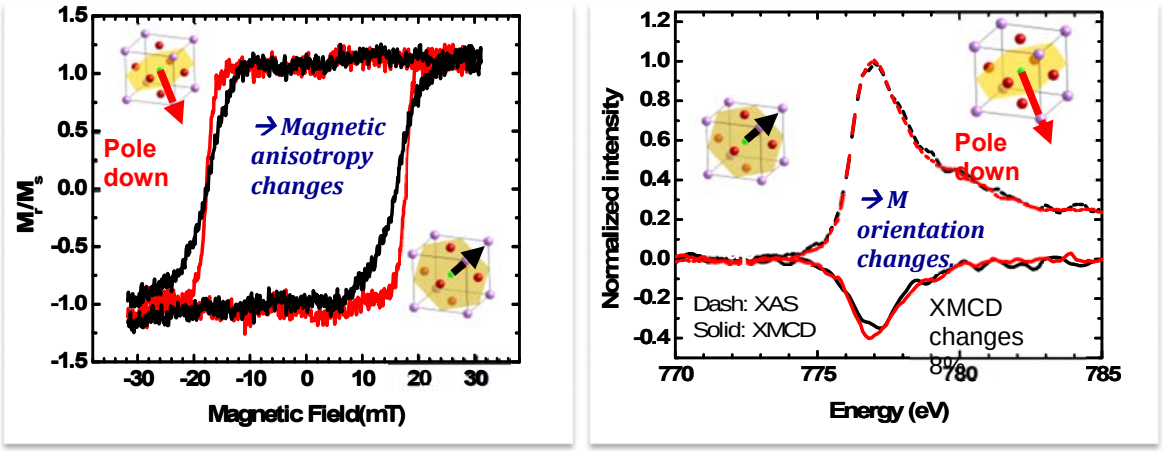

Fig. 7. XMCD and magnetic hysteresis of Co layer at 30 K.